Influence of miR-34a on myocardial apoptosis in rats with acute myocardial infarction through the ERK1/2 pathway

W.-S. BIAN¹, F.-H. TIAN², L.-H. JIANG³, Y.-F. SUN¹, S.-X. WU¹, B.-F. GAO¹, Z.-X. KANG¹, Z. ZHUO¹, X.-Z. ZHANG⁴

Abstract. – OBJECTIVE: To study the influence of micro-ribonucleic acid (miR)-34a on myocardial apoptosis in rats with acute myocardial infarction (AMI) through the extracellular signal-regulated kinase 1/2 (ERK1/2) pathway.

MATERIALS AND METHODS: A total of 24 Sprague-Dawley (SD) rats were randomly divided into sham group (n=12) and model group (n=12). The heart was exposed in the sham group, while the AMI model was established in the model group. After sampling, the morphology of myocardial tissues was observed via hematoxylin-eosin (HE) staining, the expressions of B-cell lymphoma-2 (Bcl-2) and Bcl-2 associated X protein (Bax) were detected via immunohistochemistry, and the protein expression levels of ERK1/2 and phosphorylated ERK1/2 (p-ERK1/2) were detected via Western blotting. Moreover, the expression of miR-34a was detected via quantitative Polymerase Chain Reaction (qPCR), the apoptosis was detected via terminal deoxynucleotidyl transferase-mediated dUTP nick end labeling (TUNEL), and the myocardial injury indexes were detected using a fully-automatic biochemical analyzer.

RESULTS: The morphology of myocardial tissues was normal with a complete structure in the sham group, while there was damage to myocardial tissues in different degrees in the model group. The immunohistochemical results revealed that the Bax expression was increased and the Bcl-2 expression was decreased in the model group compared with those in the sham group (p<0.05). The results of Western blotting showed that the protein expression levels of both ERK1/2 and p-ERK1/2 were significantly increased in the model group compared with those in the sham group (p<0.05). The qPCR results manifested that the expression of miR-34a in the model group markedly declined compared with that in the sham group (p<0.05). Besides, the TUNEL detection showed that the apoptosis rate in the model group was remarkably increased compared with that in the sham group (p<0.05), and the content of cardiac troponin T and creatine kinase isoenzyme in the model group was significantly higher than that in the sham group ((p<0.05)).

CONCLUSIONS: MiR-34a affects the apoptosis in AMI by regulating the ERK1/2 signaling pathway.

Key Words:

Acute myocardial infarction, MiR-34a, Apoptosis, FRK1/2

Introduction

Cardiovascular disease is one of the major diseases threatening human health, which often leads to deaths in patients. Acute myocardial infarction (AMI) is the leading cause of cardiovascular death^{1,2}, which is the myocardial necrosis caused by the acute and persistent ischemia and hypoxia of coronary artery, with precordial or substernal pain, and manifested as the sudden substernal or precordial compression pain³. Under the influence of environment and pressure, the number of AMI patients in China has increased year by year, showing a younger trend. There are at least 500,000 new cases every year, and the middle-aged men of 45-60 years old are a high-risk group for AMI. Time is life for the rescue of AMI, and restoring the myocardial blood flow earlier can preserve a little more viable myocardium, which can benefit future prevention, alleviate heart failure and preserve the cardiac function as much as possible, greatly benefiting individuals, families and society.

¹Department of Cardiovascular Medicine, Linyi No. 3 People's Hospital, Linyi, China

²Department of Emergency Internal Medicine, Linyi No. 3 People's Hospital, Linyi, China

³Department of Oncology, Linyi No. 3 People's Hospital, Linyi, China

⁴Department of Cardiovascular Medicine, Linyi People's Hospital, Linyi, China

Micro-ribonucleic acids (miRNAs) are a kind of gene regulatory factors in the organism, which are involved in the occurrence of a variety of diseases and the regulatory process of cardiovascular diseases, such as heart failure and myocardial infarction (MI). It is generally believed that miRNAs play roles mainly in cell proliferation, differentiation and apoptosis. Scholars^{4,5} have demonstrated that miRNAs degrade or inhibit the downstream messenger RNA (mRNA) through pairing with the corresponding untranslated region of the downstream target genes, thereby playing an important role in regulating transcription and pathological processes such as cell proliferation, differentiation and apoptosis. Liv et al⁶ have also shown that apoptosis is a common process regulated by miRNAs, and it has been confirmed that miR-34a is involved in a variety of pathological processes of AMI.

In the present work, the influence of miR-34a on myocardial apoptosis in AMI rats through the extracellular signal-regulated kinase 1/2 (ERK1/2) pathway was analyzed, and the possible mechanism of miR-34a in treating AMI through the ERK1/2 pathway was explored.

Materials and Methods

Laboratory Animals and Grouping

A total of 24 Sprague-Dawley (SD) male rats weighing (200±10) g were randomly divided into sham group (n=12) and model group (n=12). The rats were fed in the laboratory animal center with pure water and adequate food under a 12/12 h light/dark cycle. This study met the requirements of the Laboratory Animal Ethics Committee.

Main Reagents

Anti-B-cell lymphoma-2 (Bcl-2) antibody (Abcam, Cambridge, MA, USA), anti-Bcl-2 associated X protein (Bax) antibody (Abcam, Cambridge, MA, USA), anti-ERK1/2 antibody (Abcam, Cambridge, MA, USA), anti-phosphorylated ERK1/2 (p-ERK1/2) antibody (Abcam, Cambridge, MA, USA), immunohistochemistry kit (Maxim, Fuzhou, China), terminal deoxynucleotidyl transferase-mediated dUTP nick end labeling (TUNEL) kit (Maxim, Fuzhou, China), hematoxylin-eosin (HE) kit (Maxim, Fuzhou, China), AceQ quantitative-Polymerase Chain Reaction (qPCR) SYBR Green Master Mix Kit (Vazyme, Nanjing, China), HiScript II Q RT SuperMix For qPCR (+gDNA wiper) kit (Vazyme, Nanjing,

China), optical microscope (Leica DMI 4000B/DFC425C, München, Germany), fluorescence qPCR instrument (Applied Biosystems 7500, Foster City, CA, USA), and fully-automatic biochemical analyzer (Siemens, Berlin, Germany).

Methods

Modeling and Treatment in Each Group

After successful anesthesia via intraperitoneal injection of 2.5% pentobarbital sodium into rats (30 mg/kg), the rats were fixed on the operating table and unhaired. After skin preparation and draping with aseptic towels, the rats were connected to the electrocardiograph, the tracheal cannula was inserted between the 3rd and 4th cartilage rings, and the ventilator was also connected (tidal volume: 7 mL/kg, respiratory ratio: 1:1). A longitudinal left parasternal incision (3 cm long) was made, and the skin, muscles and fascia were cut open in turn. The 3rd and 4th ribs were cut off to fully enlarge the thoracic cavity and expose the heart. The pericardium was carefully cut using ophthalmic forceps, and the #0 silk thread was inserted between the left auricle and the arterial cone. The electrocardiogram response in the electrocardiograph was observed, and the typical ischemic electrocardiogram indicated the successful establishment of the AMI model. After that, the skin was sutured layer by layer, and the air in the thoracic cavity was discharged. After consciousness recovery, the ventilator was withdrawn, and the rats were kept warm and fed in separate cages.

In the sham group, the thoracic cavity was opened only to expose the heart, and the #0 silk thread was not inserted between the left auricle and the arterial cone. After the skin was sutured layer by layer, the rats were fed normally with normal food and pure water every day. In the model group, the AMI model was established in the above ways, and the rats were fed with normal food and pure water every day after successful modeling. All rats were executed and sampled at 7 d after the operation.

Sampling

After anesthesia, the abdominal cavity was cut open to expose the abdominal aorta, and the abdominal aortic blood was collected from each rat using disposable blood-taking needles and preserved for standby use. Then, 6 rats in each group were perfused with paraformaldehyde (Sigma-Al-

drich, St. Louis, MO, USA) and fixed. After the limbs of rats became rigid, the heart tissues were taken and fixed in paraformaldehyde for 48 h. The heart tissues were directly taken from the remaining 6 rats in each group, placed in Eppendorf tubes (EP; Eppendorf, Hamburg, Germany) and stored in an ultra-low temperature refrigerator for later use.

HE Staining

The paraffin-embedded tissues were sliced into 5 µm-thick sections, flattened in warm water at 42°C, picked up and baked to be prepared into paraffin tissue sections. Then, the sections were routinely deparaffinized with xylene solution, dehydrated with gradient alcohol, stained with hematoxylin dye at room temperature for 10 min, washed, differentiated in hydrochloric acid alcohol solution for several seconds, washed again and reacted with eosin dye for 30 s, followed by rehydration with gradient alcohol, moderate color development and sealing.

Immunohistochemistry

The paraffin-embedded tissues were sliced into 5 μm-thick sections, flattened in warm water at 42°C, picked up and baked to be prepared into paraffin tissue sections. Then, the sections were routinely deparaffinized with xylene solution, and dehydrated with gradient alcohol. The above sections were soaked in the citric acid buffer and heated repeatedly in a microwave oven 3 times (3 min/time) and braised for 5 min for full antigen retrieval. After the sections were washed, the endogenous peroxidase blocker was added dropwise onto the sections for reaction for 10 min, and the sections were washed again and sealed with goat serum for 20 min. After the goat serum was discarded, the Bax primary antibody (1:200) and Bcl-2 primary antibody (1:200) were added for incubation in the refrigerator at 4°C overnight. On the next day, the sections were washed, reacted with the secondary antibody for 10 min, fully washed again and reacted with the streptavidin-peroxidase solution for 10 min, followed by color development with diaminobenzidine (DAB), nucleus counterstaining with hematoxylin, sealing and observation.

Western Blotting

The heart tissues stored under ultra-low temperature were added with lysis buffer for an ice bath for 1 h and centrifuged at 14000 g in a centrifuge for 10 min, and the protein was quantified using bicinchoninic acid (BCA; Pierce, Waltham,

MA, USA). The absorbance value was detected using a microplate reader, the standard curves were plotted, and the protein concentration in tissues was detected. After protein denaturation, the protein in tissues was separated via sodium dodecyl sulphate-polyacrylamide gel electrophoresis (SDS-PAGE). The position of the Marker protein was observed, and the electrophoresis was terminated when the Marker protein reached the bottom of the glass plate in a straight line. The protein was transferred onto polyvinylidene difluoride (PVDF) membrane (Millipore, Billerica, MA, USA), reacted with blocking buffer for 1.5 h, and incubated with the anti-ERK1/2 primary antibody (1:1000), anti-p-ERK1/2 primary antibody (1:1000) and secondary antibody (1:1000). After the membrane was washed, the color was fully developed in a dark place using the chemiluminescence reagent for 1 min.

Quantitative-Polymerase Chain Reaction

The heart tissues stored were added with the RNA extraction reagent to extract the total RNA. Then, the total RNA extracted was reversely transcribed into cDNA using the reverse transcription kit. The reaction system was 20 μ L, and the reaction conditions are as follows: reaction at 53°C for 5 min, pre-denaturation at 95°C for 10 min, denaturation at 95°C for 10 s, annealing at 62°C for 30 s, a total of 35 cycles. The Δ Ct value was calculated first, and then the difference in the expression of the target gene was calculated. The primer sequences are shown in Table I.

TUNEL Assay

The paraffin-embedded tissues were sliced into 5 μ m-thick sections, flattened in warm water at 42°C, picked up and baked to be prepared into paraffin tissue sections. Then, the sections were routinely deparaffinized with xylene solution, and dehydrated with gradient alcohol.

 Table I. Primer sequences.

Name	Primer sequence
miR-34a	Forward primer: 5'-TGGCGATGGCAGTGTCTTAG-3' Reverse primer: 5'-GTGCAGGGTCCGAGGT-3'
GAPDH	Forward primer: 5'-ACGGCA AGTTCA ACGGCACAG-3' Reverse primer: 5'-GA AGACGCCAGTAGACTCCACGAC-3'

TdT reaction solution was added dropwise for reaction in a dark place for 1 h, and deionized water was added dropwise for incubation for 15 min to terminate the reaction. The endogenous peroxidase was inactivated with hydrogen peroxide, the working solution was added dropwise for reaction for 1 h, and the sections were washed, followed by color development with DAB, washing, sealing and observation.

Detection of Myocardial Injury Markers Using the Fully-Automatic Biochemical Analyzer

The abdominal aortic blood collected was placed in the fully-automatic biochemical analyzer to detect the content of myocardial injury markers in the serum according to the specifications and instructions of the instrument.

Statistical Analysis

Statistical Product and Service Solutions (SPSS) 20.0 software (IBM, Armonk, NY, USA) was used for statistical analysis. The *t*-test was used for the data in line with normal distribution and homogeneity of variance, corrected *t*-test for the data in line with normal distribution and heterogeneity of variance, and non-parametric test for the data not in line with normal distribution and homogeneity of variance. Rank sum test was adopted for ranked data, and chi-square test was adopted for enumeration data. A *p*-value < 0.05 was considered statistically significant.

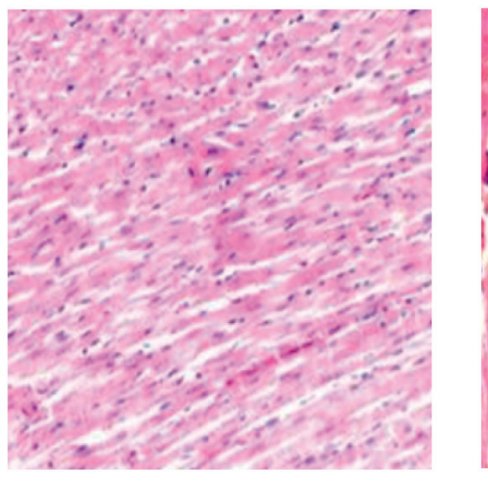
Results

Morphology of Heart Tissues Observed Via HE Staining

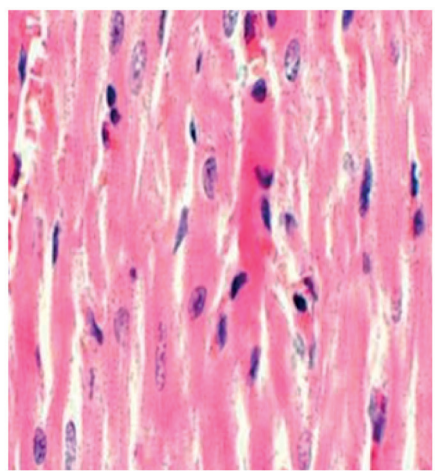
In the sham group, the heart tissues had no significant abnormal changes, the myocardial cells had normal morphology and uniform and ordered arrangement, and the myocardial fibers were regular, clear and arranged orderly. In the model group, a large number of myocardial cells were ruptured, the morphology was irregular with disordered arrangement, the nuclei were massively dissolved, more inflammatory cells could be seen, there were rupture and necrosis of myocardial fibers with irregular morphology and structure disorder, and the fibroblast proliferation and scar tissue formation were observed (Figure 1).

Immunohistochemical Detection of Bax and Bcl-2 Expression

The positive expression of Bax and Bcl-2 displayed the dark brown color. The positive expression of Bcl-2 was higher, while the positive expression of Bax was lower in the sham group. The positive expression of Bcl-2 was lower, while the positive expression of Bax was higher in the model group (Figure 2). As shown in Figure 3, the positive expression of Bcl-2 in the sham group was markedly higher than that in the model group, while the positive expression of Bax in the sham group was remarkably lower than that in the







Model group

Figure 1. Morphology of heart tissues observed *via* HE staining ($\times 200$). Note: p*<0.05 vs. sham group.

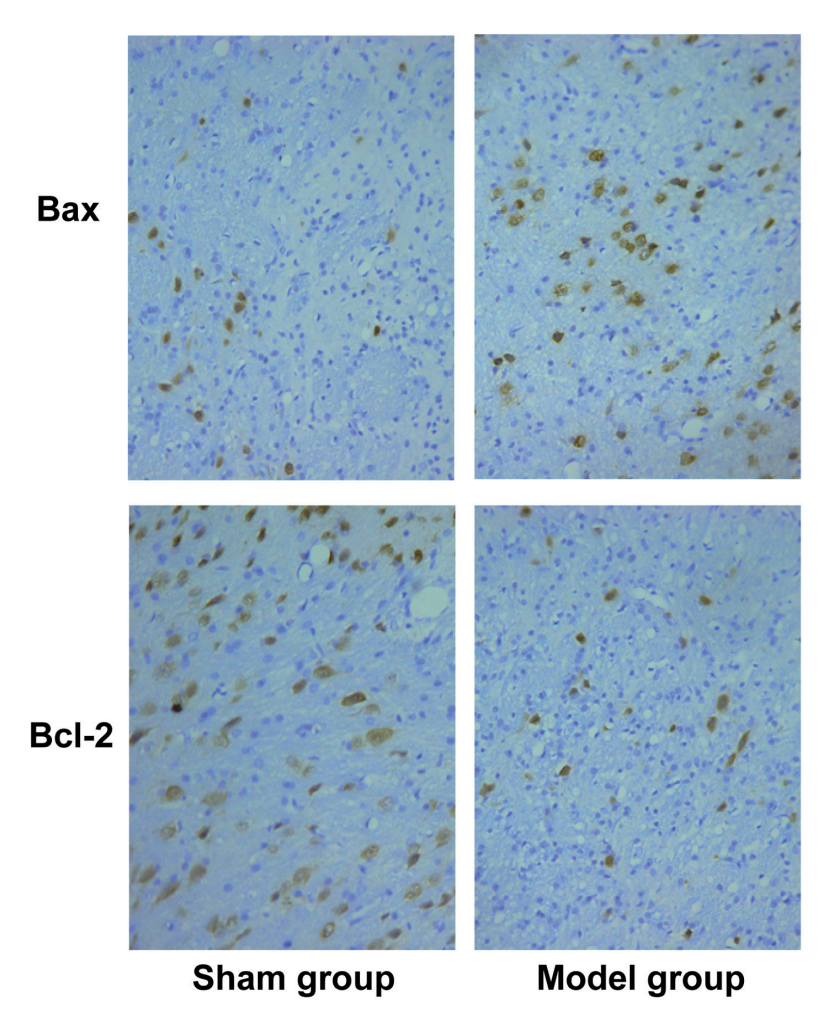


Figure 2. Immunohistochemical detection of Bax and Bcl-2 expressions.

model group, showing statistically significant differences (p<0.05).

ERK1/2 and p-ERK1/2 Protein Expressions Detected Via Western Blotting

The protein expressions of ERK1/2 and p-ERK1/2 were lower in the sham group and higher in the model group (Figure 4). The relative protein expression levels of ERK1/2 and p-ERK1/2 were markedly lower in the sham group than those in the model group, displaying statistically significant differences (p<0.05) (Figure 5).

Relative Expression Level of MiR-34a Detected Via qPCR

As shown in Figure 6, the relative expression level of miR-34a was higher in the sham group

and lower in the model group, and the difference was statistically significant (p<0.05).

Apoptosis Rate Detected Via TUNEL

As shown in Figure 7, the apoptosis rate in the sham group [(13.32±7.44)%] was markedly lower than that in the model group [(38.36±5.65)%], and there was a statistically significant difference.

Myocardial Injury Markers Detected

The content of cardiac troponin T was (0.53±0.21) ng/L in the sham group and (12.27±3.77) ng/L in the model group, and the content of creatine kinase isoenzyme was (31.78±7.63) U/L in the sham group and (118.38±17.66) U/L in the model group. It can be seen that the content of both cardiac troponin T and creatine kinase isoenzyme in the

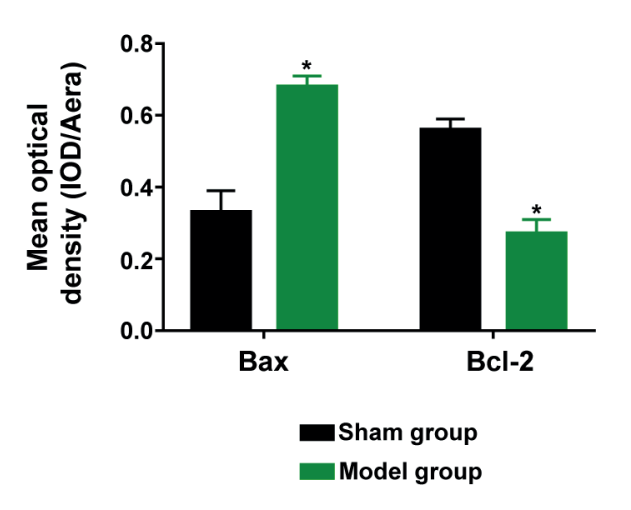


Figure 3. Mean optical density of Bax and Bcl-2 positive expression. Note: p*<0.05 vs. sham group.

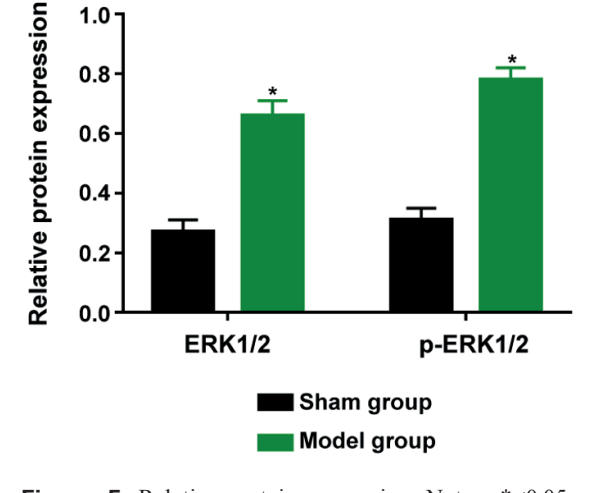


Figure 5. Relative protein expression. Note: p*<0.05 vs. sham group.

sham group was remarkably lower than that in the model group (Figure 8).

Discussion

The complex cellular and molecular mechanisms and a series of complex cascades are major factors leading to ventricular remodeling disorder after AMI7. The important pathological responses affecting ventricular remodeling after MI include myocardial apoptosis or necrosis, myocardial pathological hypertrophy and gene re-expression, and extracellular matrix metabolism disorder^{8,9}, among which myocardial apoptosis is an important pathological response after MI and plays an important role in ventricular remodeling after MI. Further studies^{10,11} have demonstrated that the excessive myocardial apoptosis after MI can lead to thickening of the non-MI region, and irregular thinning of MI region. In addition, the excessive fibroblast

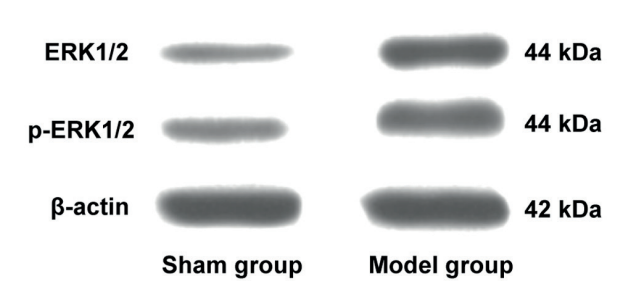


Figure 4. Protein expression detected *via* Western blotting.

proliferation and excessive deposition or degradation of extracellular matrix after MI can result in ventricular remodeling disorder after MI, affecting the cardiac function.

The ERK1/2 signaling pathway, an important cellular signal transduction pathway, has a close correlation with various responses, especially apoptosis^{12,13}. It is known that mitogen-activated protein kinase (MAPK), an important kind of serine-threonine kinase, exists widely in cells, participates in the transduction of various cellular signals, and regulates multiple downstream signaling pathways and expression of growth regulatory protein. As an important and active signaling pathway, ERK1/2 is involved in MAPK-mediated pathways, regulating various pathophysiological responses, such as cell proliferation, differentiation and apoptosis¹⁴. ERK1 and ERK2, isomers for each other, can be activated by a variety of upstream molecules, including growth factors and endothelin, and phosphorylated, thus activating other downstream kinases, phosphorylating cytoskeletal components, and activating downstream substrates to transmit information, ultimately activating multiple downstream signaling pathways^{15,16}. In the present work, it was found that the expression levels of ERK1/2 and p-ERK1/2 were markedly increased in the heart tissues of MI, indicating that multiple pathological responses after MI lead to the increase in abnormal expression of ERK1/2 and its phosphorylation. At the same time, in heart tissues of MI, the expression of Bax was significantly increased, while the

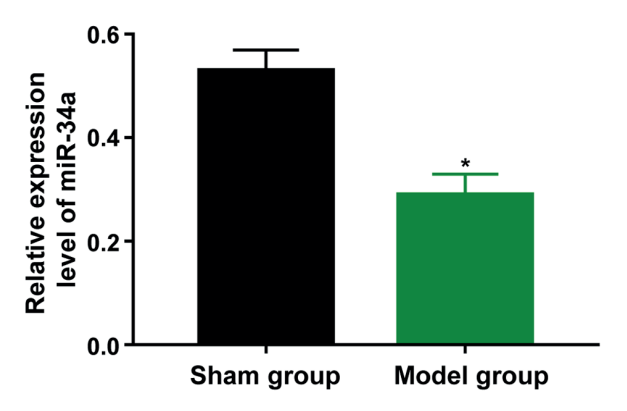


Figure 6. Relative expression level of miR-34a. Note: p*<0.05 vs. sham group.

expression of Bcl-2 was remarkably decreased, and both apoptosis rate and levels of myocardial injury markers were markedly increased. The above results indicate that Bax and Bcl-2, as downstream effectors of the ERK1/2 signaling pathway, are regulated after MI, and the ERK1/2 signaling pathway is activated, the ERK1/2 expression is increased and its phosphorylation level is remarkably increased after MI, thereby realizing cellular signal transduction, regulating the abnormal expression of downstream Bax and Bcl-2, leading to massive myocardial apoptosis and aggravating myocardial injury.

As a member of the non-coding RNA family, miR-34a has been proved to be able to regulate apoptosis, which, in particular, can increase cancer cell apoptosis, thus inhibiting cancer^{17,18}. According to further studies^{19,20}, Bax and Bcl-2 that have close correlations with apoptosis are

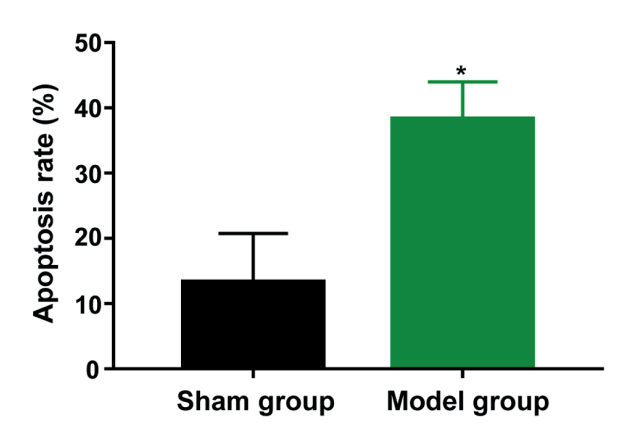


Figure 7. Apoptosis rate in each group. Note: p*<0.05 vs. sham group.

direct targets of miR-34a, and miR-34a can directly regulate the gene and protein expressions of Bax and Bcl-2, controlling apoptosis. The results of this work revealed that the expression level of miR-34a significantly declined, and the expression of Bax was markedly increased, while the expression of Bcl-2 was remarkably decreased in myocardial tissues of AMI rats, indicating that the abnormal expression of miR-34a may lead to the abnormal expressions of Bax and Bcl-2, thus promoting myocardial apoptosis. At the same time, considering the activation of the ERK1/2 signaling pathway and its role in the abnormal expression of Bax and Bcl-2, it is concluded that miR-34a regulates the myocardial apoptosis after AMI through the ERK1/2 pathway.

Conclusions

We found that miR-34a affects the apoptosis in rats with AMI by regulating the ERK1/2 signaling pathway.

Conflict of Interest

The Authors declare that they have no conflict of interest.

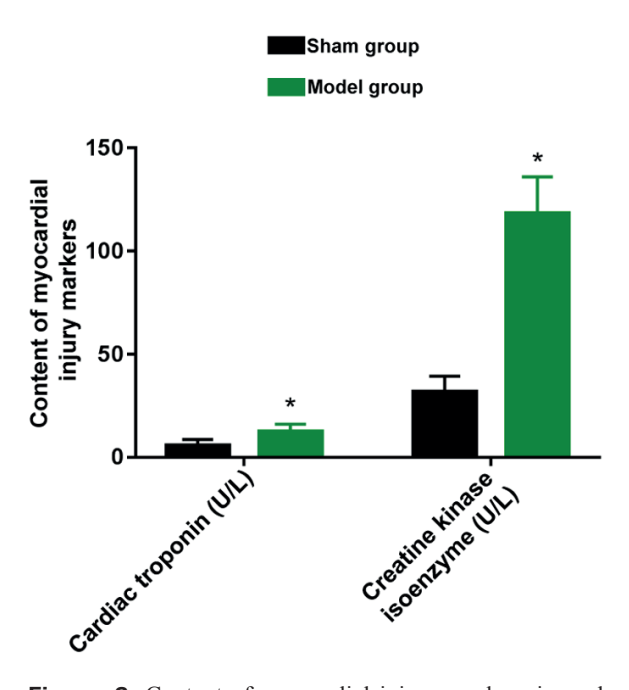


Figure 8. Content of myocardial injury markers in each group. Note: p*<0.05 vs. sham group.

3040

References

- WESTMAN PC, LIPINSKI MJ, LUGER D, WAKSMAN R, BO-NOW RO, WU E, EPSTEIN SE. Inflammation as a driver of adverse left ventricular remodeling after acute myocardial infarction. J Am Coll Cardiol 2016; 67: 2050-2060.
- Mehta LS, Beckie TM, DeVon HA, Grines CL, Kru-MHOLZ HM, JOHNSON MN, LINDLEY KJ, VACCARINO V, Wang TY, Watson KE, Wenger NK. Acute myocardial infarction in women: a scientific statement from the american heart association. Circulation 2016; 133: 916-947.
- NICCOLI G, SCALONE G, LERMAN A, CREA F. Coronary microvascular obstruction in acute myocardial infarction. Eur Heart J 2016; 37: 1024-1033.
- ZENG Y, YI R, CULLEN BR. Recognition and cleavage of primary microRNA precursors by the nuclear processing enzyme Drosha. EMBO J 2005; 24: 138-148.
- LEE Y, AHN C, HAN J, CHOI H, KIM J, YIM J, LEE J, PROVOST P, RADMARK O, KIM S, KIM VN. The nuclear RNase III Drosha initiates microRNA processing. Nature 2003; 425: 415-419.
- LIU K, HUANG J, XIE M, YU Y, ZHU S, KANG R, CAO L, TANG D, DUAN X. MIR34A regulates autophagy and apoptosis by targeting HMGB1 in the retinoblastoma cell. Autophagy 2014; 10: 442-452.
- 7) O'Donoghue ML, Glaser R, Cavender MA, Aylward PE, Bonaca MP, Budaj A, Davies RY, Dellborg M, Fox KA, Gutierrez JA, Hamm C, Kiss RG, Kovar F, Kuder JF, Im KA, Lepore JJ, Lopez-Sendon JL, Ophuis TO, Parkhomenko A, Shannon JB, Spinar J, Tanguay JF, Ruda M, Steg PG, Theroux P, Wiviott SD, Laws I, Sabatine MS, Morrow DA. Effect of Iosmapimod on cardiovascular outcomes in patients hospitalized with acute myocardial infarction: a randomized clinical trial. JAMA 2016; 315: 1591-1599.
- SHI ZY, LIU Y, DONG L, ZHANG B, ZHAO M, LIU WX, ZHANG X, YIN XH. Cortistatin improves cardiac function after acute myocardial infarction in rats by suppressing myocardial apoptosis and endoplasmic reticulum stress. J Cardiovasc Pharmacol Ther 2016; 1074248416644988.
- Li T, Wei X, Evans CF, Sanchez PG, Li S, Wu ZJ, Griffith BP. Left ventricular unloading after acute myocardial infarction reduces MMP/JNK associated apoptosis and promotes FAK cell-survival signaling. Ann Thorac Surg 2016; 102: 1919-1924.

- 10) ZHANG Y, LI C, MENG H, GUO D, ZHANG Q, LU W, WANG Q, WANG Y, TU P. BYD ameliorates oxidative stress-induced myocardial apoptosis in heart failure post-acute myocardial infarction via the P38 MAPK-CRYAB signaling pathway. Front Physiol 2018; 9: 505.
- CHEN H, XU Y, WANG J, ZHAO W, RUAN H. Baicalin ameliorates isoproterenol-induced acute myocardial infarction through iNOS, inflammation and oxidative stress in rat. Int J Clin Exp Pathol 2015; 8: 10139-10147.
- Lu Z, Xu S. ERK1/2 MAP kinases in cell survival and apoptosis. IUBMB Life 2006; 58: 621-631.
- 13) Romano G, Acunzo M, Garofalo M, Di Leva G, Cascione L, Zanca C, Bolon B, Condorelli G, Croce CM. MiR-494 is regulated by ERK1/2 and modulates TRAIL-induced apoptosis in non-small-cell lung cancer through BIM down-regulation. Proc Natl Acad Sci U S A 2012; 109: 16570-16575.
- 14) DHINGRA S, SHARMA AK, SINGLA DK, SINGAL PK. p38 and ERK1/2 MAPKs mediate the interplay of TNF-alpha and IL-10 in regulating oxidative stress and cardiac myocyte apoptosis. Am J Physiol Heart Circ Physiol 2007; 293: H3524-H3531.
- 15) ZHANG K, DING W, SUN W, SUN XJ, XIE YZ, ZHAO CQ, ZHAO J. Beta1 integrin inhibits apoptosis induced by cyclic stretch in annulus fibrosus cells via ERK1/2 MAPK pathway. Apoptosis 2016; 21: 13-24.
- 16) Li R, Zhang LM, Sun WB. Erythropoietin rescues primary rat cortical neurons from pyroptosis and apoptosis via Erk1/2-Nrf2/Bach1 signal pathway. Brain Res Bull 2017; 130: 236-244.
- 17) Li Z, Liu ZM, Xu BH. A meta-analysis of the effect of microRNA-34a on the progression and prognosis of gastric cancer. Eur Rev Med Pharmacol Sci 2018; 22: 8281-8287.
- 18) HUANG Q, ZHENG Y, OU Y, XIONG H, YANG H, ZHANG Z, CHEN S, YE Y. miR-34a/Bcl-2 signaling pathway contributes to age-related hearing loss by modulating hair cell apoptosis. Neurosci Lett 2017; 661: 51-56.
- 19) YAN S, WANG M, ZHAO J, ZHANG H, ZHOU C, JIN L, ZHANG Y, QIU X, MA B, FAN Q. MicroRNA-34a affects chondrocyte apoptosis and proliferation by targeting the SIRT1/p53 signaling pathway during the pathogenesis of osteoarthritis. Int J Mol Med 2016; 38: 201-209.
- FARSHCHIAN M, NISSINEN L, GRENMAN R, KAHARI VM. Dasatinib promotes apoptosis of cutaneous squamous carcinoma cells by regulating activation of ERK1/2. Exp Dermatol 2017; 26: 89-92.